Scientific Reports

https://doi.org/10.1038/s41598-026-56263-5

Article in Press

Sporulation generates stress-dependent phenotypic variability in the heterothallic industrial *Saccharomyces cerevisiae* Ethanol Red

Received: 9 April 2026

Accepted: 29 May 2026

Published online: 13 June 2026

Cite this article as: Paulon V., Gupte A.P., Stojkov K. *et al.* Sporulation generates stress-dependent phenotypic variability in the heterothallic industrial *Saccharomyces cerevisiae* Ethanol Red. *Sci Rep* (2026). https://doi.org/10.1038/s41598-026-56263-5

Viviana Paulon, Ameya Pankaj Gupte, Katarina Stojkov, Chiara Ruspi, Debora Casagrande Pierantoni, Marina Basaglia, Gianluigi Cardinali, Lorenzo Favaro & Laura Corte

We are providing an unedited version of this manuscript to give early access to its findings. Before final publication, the manuscript will undergo further editing. Please note there may be errors present which affect the content, and all legal disclaimers apply.

If this paper is publishing under a Transparent Peer Review model then Peer Review reports will publish with the final article.

ARTICLE IN PRESS

© The Author(s) 2026. **Open Access** This article is licensed under a Creative Commons Attribution-NonCommercial-NoDerivatives 4.0 International License, which permits any non-commercial use, sharing, distribution and reproduction in any medium or format, as long as you give appropriate credit to the original author(s) and the source, provide a link to the Creative Commons licence, and indicate if you modified the licensed material. You do not have permission under this licence to share adapted material derived from this article or parts of it. The images or other third party material in this article are included in the article's Creative Commons licence, unless indicated otherwise in a credit line to the material. If material is not included in the article's Creative Commons licence and your intended use is not permitted by statutory regulation or exceeds the permitted use, you will need to obtain permission directly from the copyright holder. To view a copy of this licence, visit http://creativecommons.org/licenses/by-nc-nd/4.0/.

ARTICLE IN PRESS

Sporulation generates stress-dependent phenotypic variability in the heterothallic industrial *Saccharomyces cerevisiae* Ethanol Red

Viviana Paulon[a], Ameya Pankaj Gupte[a], Katarina Stojkov[b], Chiara Ruspi[b], Debora Casagrande Pierantoni[b,d], Marina Basaglia[a], Gianluigi Cardinali[b,d], Lorenzo Favaro[a,c*] and Laura Corte[b,d]

[a] Waste to Bioproducts-Lab, Department of Agronomy Food Natural Resources Animals and Environment (DAFNAE), Università di Padova, Agripolis, Viale dell'Università 16, 35020 Legnaro, PD, Italy viviana.paulon@unipd.it, ameyapankaj.gupte@unipd.it, marina.basaglia@unipd.it, lorenzo.favaro@unipd.it

[b] Department of Pharmaceutical Sciences, University of Perugia, Borgo XX Giugno 74, 06121, Perugia, Italy katarina.stojkov@dottorandi.unipg.it, chiara.ruspi@gmail.com, debora.casagrandepierantoni@unipg.it, gianluigi.cardinali@unipg.it, laura.corte@unipg.it

[c] Department of Microbiology, Stellenbosch University, Private Bag X1, Matieland 7602, South Africa

[d] CEMIN, Centre of Excellence on Nanostrucured Innovative Materials, Department of Chemistry, Biology and Biotechnology, University of Perugia, Via Elce di Sotto 8, 06123 Perugia, Italy

*__Corresponding author__: Lorenzo Favaro lorenzo.favaro@unipd.it, ORCID ID 0000-0002-5650-4422

ARTICLE IN PRESS

Abstract

The industrial yeast *Saccharomyces cerevisiae* Ethanol Red is widely used in large-scale bioethanol production and is generally considered phenotypically stable because of its heterothallic diploid background. Here, we investigated whether extensive sporulation of this highly domesticated strain could generate functional diversification without genetic engineering. Thirty monosporal cultures (MSCs) were randomly selected and profiled for growth kinetics, CFU-based cultivability and Fourier-Transform Infrared (FTIR) fingerprints under three industrially relevant stressors, namely furfural (3 g L^{-1}), formic acid (3 g L^{-1}) and

ARTICLE IN PRESS

sodium chloride (50 g L^{-1}), applied at the half maximal effective concentration (EC_{50}) of the parental strain. Sporulation generated reproducible phenotypic variability among MSCs, with the greatest divergence observed under furfural stress. Sodium chloride caused moderate differences, whereas formic acid was associated with reduced cultivability across the tested MSCs. FTIR analysis highlighted stressor-specific biochemical fingerprints, with the widest dispersion observed under furfural exposure, consistent with the marked phenotypic heterogeneity detected at the physiological level. Furfural exposure generated spectral signatures compatible with envelope perturbation and redox imbalance, whereas formic acid affected protein- and phospholipid-associated regions and sodium chloride elicited membrane–protein adjustments linked to osmotic adaptation. Overall, sporulation revealed hidden adaptive potential, supporting classical non-GMO diversification as a promising strategy for strain improvement in bioethanol and lignocellulosic biorefinery applications.

Keywords *Saccharomyces cerevisiae*, bioethanol, lignocellulosic inhibitors, formic acid, furfural, sodium chloride, heterothallism, sporulation, non-GMO strategies, stress response, FTIR.

ARTICLE IN PRESS

Graphical abstract

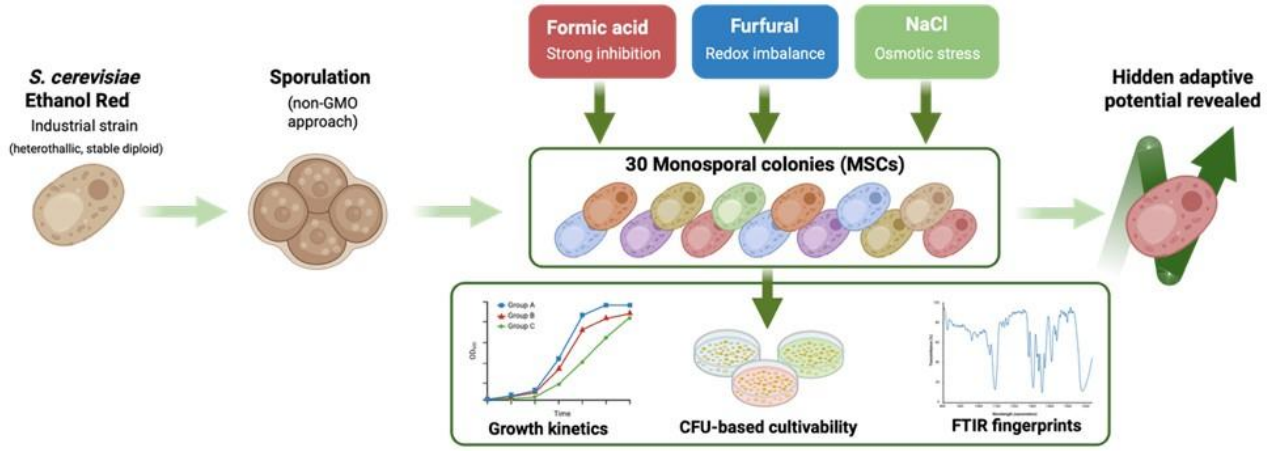

1. Introduction

ARTICLE IN PRESS

Beyond its central role as a eukaryotic model organism, *Saccharomyces cerevisiae* is a cornerstone of modern industrial biotechnology, particularly in bioethanol production and other large-scale fermentation processes [1–3]. Centuries of domestication under human-driven selective pressures have shaped industrial yeast lineages toward rapid sugar utilization, high ethanol productivity and tolerance to multiple environmental stresses, often accompanied by reduced outcrossing, clonal propagation, and lineage-specific restructuring of genetic diversity [4,5]. Therefore, many industrial strains currently in use are highly specialized and predominantly clonally propagated, often displaying reduced sexual competence and lineage-specific genomic signatures of domestication. With the advancement of microbiological knowledge applied to fermentation processes, bakers and brewers recognized the pivotal role of *S. cerevisiae* strains and began selecting pure cultures. This practice contributed to the standardization of industrial fermentations and to a narrowing of the strain repertoire used in many applications. Consequently, many strains currently employed in industrial applications, particularly in bioethanol, wine, and beer fermentations, remain in use because of historical adoption, process compatibility and proven robustness, rather than systematic re-evaluation under updated selection criteria [6]. Moreover, the evolving demands of consumers and industrial stakeholders highlight that, despite their long history of domestication, industrial yeast strains still offer considerable scope for further improvement and optimization.

Non-genetically modified (non-GMO) strategies remain highly attractive for the improvement of industrial yeast strains, especially in applications related to food, feed, and biofuels, where regulatory constraints and public acceptance limit the deployment of genetically engineered organisms. Within this framework, classical genetic approaches, including sporulation and selection, have been proposed as tools to reveal and reshuffle standing variation within industrial strains [7,8], thereby generating phenotypic diversity and potentially uncovering hidden or cryptic variability.

ARTICLE IN PRESS

Compared with self-cloning or targeted genetic engineering strategies, sporulation-based diversification exploits naturally occurring meiotic segregation and does not require the introduction of exogenous DNA or induced mutagenesis [9]. Moreover, unlike the direct selection of resistant derivatives under selective pressure, sporulation may provide access to broader combinations of segregating traits, making it a useful exploratory approach for phenotypic screening in industrial yeast backgrounds [10].

In principle, however, the extent of variability that can be generated through sporulation critically depends on the ploidy, heterozygosity and overall genetic architecture of the parental strain [10-12]. In a diploid industrial strain such as the widely used bioethanol yeast *S. cerevisiae* Ethanol Red, sporulation followed by germination would be expected to yield limited phenotypic variability if the parental genome were largely homozygous, because only a restricted amount of genetic variation would be available for meiotic segregation [13,14]. Consequently, spore-derived populations from such strains are often assumed to display limited phenotypic segregation, at least for many traits under standard conditions. Contrary to this expectation, in the present study we demonstrate that extensive sporulation of *S. cerevisiae* Ethanol Red generates a measurable and reproducible phenotypic variability under industrially relevant stress conditions typical of bioethanol and biorefinery processes (ie, sodium chloride, furfural, and formic acid). Improved tolerance to such stressors resulted in better ethanol performances and/or shorter lag phase. For instance, mutant strains of S. cerevisiae via ionizing radiation combined with adaptive laboratory evolution [15] displayed a much shorter lag phase (-40%). Similarly, the enhanced salt tolerance in S. cerevisiae has been linked to nearly 1-2-fold ethanol productivity and yields [16]. Recent studies demonstrated that S. cerevisiae strains resistant to formic acid maintain high fermentative performance under inhibitory conditions with improved growth and ethanol productivity by at least 50 and 40%, respectively [18, 19]. In this work, specifically, variability emerged in response to sodium chloride, furfural, and

ARTICLE IN PRESS

formic acid, three key stressors associated with bioethanol and biorefinery processes [19-21]. Both growth responses and FTIR metabolomic fingerprints of selected monosporal colonies displayed substantial variability. These findings suggest that sporulation can uncover functionally relevant diversity even in highly domesticated, heterothallic industrial yeasts, raising important questions about the contribution of cryptic genetic variation, meiotic segregation and stress-dependent phenotypic expression.

By systematically assessing the stress tolerance of spore-derived isolates, this work provides new insights into the potential of classical, non-GMO approaches to reveal exploitable phenotypic variation in established industrial yeast strains, with possible implications for strain improvement strategies in biofuel and bioproduct applications.

2. Materials and Methods

2.1 Cultures, media and cultivation conditions

The industrial *Saccharomyces cerevisiae* strain (Ethanol Red) was adopted in this study. Unless otherwise specified, reagents were purchased from Sigma-Aldrich (St. Louis, MO, USA). The strain was stored as glycerol stock (20% v/v) at -80°C. For routine cultivation, 5 µL of glycerol stock was streaked onto YPD agar plates containing yeast extract (10 g L^{-1}), peptone (20 g L^{-1}), glucose (20 g L^{-1}), agar (15 g L^{-1}; Liofilchem S.r.l., Roseto degli Abruzzi, Italy) and incubated at 30°C for 48h. Sporulation ability was assessed by cultivation on McClary's acetate medium (MAM; glucose 1 g L^{-1}, potassium chloride 1.8 g L^{-1}, yeast extract 2.5 g L^{-1}, sodium acetate trihydrate 8.2 g L^{-1}) and modified sporulation medium (MSM; potassium acetate 10 g L^{-1}, yeast extract 0.5 g L^{-1}, glucose 1 g L^{-1}, agar 15 g L^{-1}; Liofilchem S.r.l., Roseto degli Abruzzi, Italy), incubated at 30°C for 7-21 days [22]. All media were sterilized by autoclaving at 121°C for 20 min (Fedegari FVG2, Fedegari Group, Albuzzano, Italy).

2.2 Sporulation assay

ARTICLE IN PRESS

Sporulation was performed according to Gupte et al. [7] with minor modifications. Briefly, a single colony grown on YPD agar was inoculated into 5 mL of YPD broth in a 15 mL tube and incubated at 30°C for 16h under orbital shaking. Cells were harvested by centrifugation (4500 × *g*, 5 min), and the resulting pellet was washed with sterile saline solution (NaCl, 9 g L^{-1}). Washed cells were resuspended in 0.5 mL saline solution. To identify the optimal sporulation medium, 0.1 mL of the cell suspension was spread onto both MAM and MSM agar plates to obtain lawn growth. Plates were sealed with Parafilm (Bemis Company, Inc., USA), to prevent moisture loss and incubated at 30°C for 7-21 days. Sporulation was monitored by weekly microscopic observations. The number of dyads, triads and tetrads was quantified using a Thoma counting chamber (Marienfeld, Germany). Sporulation efficiency was calculated as described by Budroni et al. [23].

2.3 Isolation of monosporal colonies (MSCs)

Monosporal colonies (MSCs) were obtained following a modified version of the ascospore isolation protocol described by Bahalul et al. [24], omitting the diethyl ether step. Sporulated biomass from MSM plates was scraped and resuspended in sterile demineralized water to obtain a high-density ascus suspension. The suspension was heat-treated at 65 °C for 10 minutes to kill vegetative cells. Ascus wall digestion was then performed with Zymolyase (Zymolyase-100T, ICN) at a final concentration of 100 U mL^{-1} in 1 M sorbitol, following Bahalul et al. [18] with an extended incubation time of 1 h. Mechanical disruption was subsequently achieved by vortexing using a ZX3Vortex Mixer (VELP Scientifica, Usmate Velate, Italy) in the presence of sterile glass beads (400-600 µm). The resulting spore suspension was examined by light microscopy following methylene blue (MB) staining to evaluate the presence of viable and non-viable asci or vegetative cells. MB uptake was interpreted as loss of cell membrane integrity. The suspension was then diluted and plated on YPD agar plates supplemented with 5% (w/v) glucose (YPD 5%). Colonies recovered on YPD

ARTICLE IN PRESS

plates were designated as MSCs. Up to 100 MSCs were cryopreserved as glycerol stocks (20% v/v) at -80 °C. For phenotypic verification, MSCs were re-cultured on YPD 5%, transferred to MSM plates and incubated at 30°C for 7-21 days to evaluate their ability to sporulate upon re-induction.

2.4 Experimental validation of heterothallism in the parental strain

The heterothallic nature of parental strain (PS) was initially assessed by microscopic observation of MSCs to evaluate ascus formation as well as by genomic insights on HO locus structure and nature. Microscopic observation of monosporal cultures derived from the parental strain did not reveal recurrent ascus formation after re-inoculation on sporulation medium, supporting a heterothallic life cycle. The absence of asci formation was taken as indicative of a heterothallic phenotype. Genomic analyses were then performed to confirm heterothallism at the molecular level. Whole-genome sequencing of the parental strain has been previously carried out using a hybrid strategy combining Illumina short-read sequencing and Oxford Nanopore MinION long-read sequencing [25]. Assemblies from both platforms were integrated to generate a high-quality genome assembly [17]. The assembled sequence was screened by nBLAST for the presence of the HO gene, which is responsible for mating-type switching in homothallic strains. The occurrence of a truncated or incomplete HO sequence in the parental strain was used to further confirm its heterothallic life cycle.

ARTICLE IN PRESS

2.5 Phenotypic characterization of monosporal cultures

The phenotypic variability among MSCs was evaluated by growth profiling. Thirty MSCs were randomly selected and pre-cultured in Synthetic Defined medium (SD) containing glucose (20 g L^{-1}) and yeast nitrogen base without amino acids (YNB, 6.7 g L^{-1}; Difco Laboratories, USA) at 30°C for 16 h. Pre-cultures were then inoculated into fresh SD medium at initial OD_{600} = 0.1 and a final volume of 200 µL per well. Growth assays were run in triplicate in 96-well flat-bottom plates using a Spark 10M plate reader (TECAN, Austria). Optical density was

ARTICLE IN PRESS

monitored over time, and growth curves were generated using the Pyphe-growthcurves pipelines.

2.6 Determination of EC_{50} values for the heterothallic parental strain

The parental strain was pre-cultured in SD medium (glucose 20 g L^{-1}; YNB 6.7 g L^{-1}) at 30°C for 16 h and then inoculated into fresh SD medium supplemented with increasing concentration of the selected stressors (sodium chloride, furfural and formic acid) to a final OD_{600} = 0.1 in a final volume of 200 µL per well. Growth assays were performed in triplicate in 96-well plates using a Spark 10 M plate reader (TECAN, Austria).

Formic acid, furfural and sodium chloride were selected as representative inhibitory compounds commonly encountered in industrial bioethanol fermentations. Concentration ranges were defined based on their known inhibitory effects on yeast growth. Formic acid was evaluated at 1-4.3 g L^{-1}, as it can arise from the degradation of HMF and furfural under acidic conditions [26,27]. Furfural, representing furan derivatives commonly generated during biomass pre-treatment processes, was tested at 0.1-5 g L^{-1} [28]. Sodium chloride was included as an osmotic stressor and tested at 15-90 g L^{-1}. Cultures were incubated at 30°C under static conditions for 48 h, with optical density measurements recorded at 60 min intervals. To minimize evaporation, the instrument lid and humidity cassette were used throughout the experiment. Growth curves were generated using the Pyphe-growthcurves pipeline, and growth parameters (max_slope, t_max, and Lag) were extracted as described above. The half maximal effective concentration (EC_{50}) was determined for each stressor based on the growth-curve analysis and the corresponding derived parameters.

2.7 Growth assessment of MSCs under stress conditions at EC_{50} concentration

Thirty MSCs derived from the sporulation of the parental strain were randomly selected from the preserved monosporal collection following a conservative sampling strategy previously adopted for sporulation-derived yeast populations [7]. This approach was intended to obtain an

ARTICLE IN PRESS

exploratory subset while limiting the repeated analysis of potentially redundant isolates. The sample size was chosen because extensive phenotypic diversification was not expected a priori in the highly domesticated and presumed genetically stable Ethanol Red background. The selected MSCs were pre-cultured in SD medium at 30°C for 24 h. Growth assays were performed in triplicate in 96-well plates. Each culture was inoculated at an initial OD_{600} = 0.1 into fresh SD medium supplemented with the stressor-specific EC_{50} concentration previously determined for the parental strain, in a final volume of 200 µL per well. Cultures were incubated for 24 h under the same conditions used for the parental strain growth assay (30 °C, static incubation, OD_{600} readings every 60 min) and growth parameters were extracted using the Pyphe-growthcurves pipeline (**Table S1**). For furfural and sodium chloride, six MSCs were selected for more detailed growth and stress-response characterization based on their final OD_{600} values relative to the parental strain: two with significantly higher growth, two with significantly lower growth and two with growth comparable to that of the parental strain. Differences in final OD_{600} values were assessed using Student's t-test, with significance thresholds set at $p < 0.01$ and $p < 0.001$. For formic acid, since all MSCs displayed lower final OD_{600} values than the parental strain, the six MSCs selected were those with growth values closest to the parental phenotype.

ARTICLE IN PRESS

2.8 FTIR bioassay and viability assessment

Fourier Transform Infrared (FTIR) spectroscopy was employed to profile the stress-associated biochemical changes in the selected MSCs cultures exposed to formic acid, furfural or sodium chloride, using the parental strain as a reference [29,30]. Precultures were inoculated at OD_{600} = 0.1 in 100 mL of YNB medium (6.7 g L^{-1}; Difco Laboratories, USA) supplemented with glucose (20 g L^{-1}) and incubated at 30°C (FOC Connect cooled incubator, VELP Scientifica, Usmate Velate, Italy) with orbital shaking at 120 rpm using an Unimax 1010 orbital shaker (Heidolph Instruments GmbH & Co. KG, Schwabach, Germany) for 16-18 h. For stress assays,

ARTICLE IN PRESS

MSCs and parental cultures were inoculated at OD_{600} = 12 in the same medium and incubated for 4 h to allow metabolic adaptation prior to stress exposure. Stressors were then added to final concentrations of 3 g L^{-1} (formic acid and furfural) and 50 g L^{-1} (NaCl), and incubation was continued for additional 4 h at 30 °C with shaking at 120 rpm. Control samples were processed in parallel by continuing incubation for additional 4 h under identical conditions, but without the addition of any stressor. All experiments were performed in biological triplicate. At the end of the incubation, whole-cell pellets were collected by centrifugation (4500 × *g*, 5 min), washed twice with distilled sterile water and re-suspended in 5 mL HPLC (High-Performance Liquid Chromatography) grade water to the final concentration of OD_{600} = 20, prior to FTIR analysis. FTIR spectra were acquired in transmission mode using a TENSOR 27 spectrometer equipped with an HTS-XT screening module (Bruker Optics GmbH, Ettlingen, Germany). Spectra were recorded in the 3200-900 cm^{-1} range at a resolution of 4 cm^{-1} sampling 256 scans per sample.

From each suspension, 105 µL was collected for three independent FTIR readings (35 µL each) [31], while 100 µL were serially diluted to assess viability by plate counting on YPD agar supplemented with chloramphenicol (0.5 g L^{-1}). Mortality (%) was calculated as [1 – (CFU_{test} / $CFU_{control}$)] x 100. Stress tolerance, *i.e.* cultivability under stress, was reported (i) as percentage mortality for each culture and (ii) as relative cultivability, expressed as fold change (FC), calculated both for each culture [**FC** = CFU_{test} / $CFU_{control}$] and for each MSC relative to the parental strain [**FC** = CFU_{MSC} / $CFU_{parental}$]. An FC = 1 indicates no change, FC > 1 increased cultivability and FC < 1 decreased cultivability (**Table 1**, **Table 2**).

Overall, the experimental approaches described in paragraphs 2.7 and 2.8 were designed to assess different components of the stress response. The growth assay described in paragraph 2.7 evaluated the ability of MSCs to adapt and resume growth over prolonged cultivation under stress conditions, whereas the FTIR bioassay and viability assessment described in paragraph

ARTICLE IN PRESS

2.8 specifically measured short-term survival and cultivability after acute stress exposure at high cell density.

2.9 Statistical Analyses

2.9.1 Growth parameters data analysis

Optical density was recorded over time and growth curves were generated using the Pyphe-growthcurves pipeline as described by Kamrad et al. [32]. From each curve, growth parameters including maximum growth rate (max_slope), time at maximum growth rate (t_max) and lag phase duration (Lag) were extracted using the same computational framework. Parameter extraction was performed on biological triplicates and mean values were calculated for downstream analyses. Phenotypic variation among MSCs was investigated by Principal Component Analysis (PCA) using R software [33]. PCA was applied to the matrix of extracted growth parameters after centering and scaling of variables to account for differences in parameter magnitude. The analysis was used to reduce dimensionality and to identify the main sources of variance associated with strain-dependent growth behavior. PCA score plots were generated using the ggplot2 package, and samples were grouped according to strain identity and experimental condition to visualize clustering patterns and dispersion.

ARTICLE IN PRESS

2.9.2 FTIR Spectral Data

FTIR spectra were pre-processed using OPUS software version 6.5 (Bruker Optics GmbH, Ettlingen, Germany) by baseline and vector normalization and transferred to MS Excel for further analysis in R [33]. Mean spectra were obtained by averaging three independent technical replicates for each biological replicate (**Tables S2, S3, S4**). Significant Wavelengths Analysis (SWA) script was then carried out on the FTIR spectra by partitioning it into four spectral regions (W1: 2800-3200 cm^{-1}; W2: 1500-1800 cm^{-1}; W3: 1200-1500 cm^{-1} and W4: 900-1200 cm^{-1}), following the procedure described by Corte et al. [34]. For each tested condition, spectra of each MSC were compared with those of the parental strain by applying a

ARTICLE IN PRESS

two-tailed Student's T-test to each wavelength independently within each spectral region. To reduce the likelihood of false-positive results arising from simultaneous statistical testing across a large number of wavenumbers, *p*-values were corrected for multiple testing using the Benjamini–Hochberg false discovery rate (FDR) procedure. Wavenumbers were considered significant when FDR-adjusted $p < 0.01$. Bubble plots were then generated by using the ggplot2 function to visualize, for each stress condition, the number of significantly different wavelengths observed in the parental-MSC comparisons across the six selected MSCs.

Significant wavenumbers with FDR-adjusted $p < 0.05$ were then grouped into contiguous intervals and assigned to predefined spectral windows. Significant peaks were defined as the wavenumber with maximum intensity within each interval and assigned to the bond vibrations listed in **Table 2**. Mean spectra were plotted with significant peaks marked (**Figure S1, S2, S3**).

PCA was conducted using the *prcomp* function with centering and scaling enabled. The analysis was performed on the full spectral matrix to reduce dimensionality and identify major sources of variance associated with treatment effects. PCA score plots were generated with ggplot2, where samples were colored according to treatment group and technical/biological replicates were retained to preserve within-group variability. Ninety-five percent confidence ellipses were computed using a multivariate normal model to visualize group dispersion.

ARTICLE IN PRESS

3. Results and Discussion

3.1 Growth response under stress

Increasing concentration of furfural (1-5 g L^{-1}), formic acid (1- 4.3 g L^{-1}) and sodium chloride (15-90 g L^{-1}) produced a clear dose-dependent inhibition of growth in the parental *S. cerevisiae* Ethanol Red strain. For each compound, the half-maximal effective concentration (EC_{50}) was determined, defined as the dose causing marked but incomplete growth inhibition over 24 h. Under the EC_{50} concentration, the 30 randomly selected MSCs revealed a broad distribution of

ARTICLE IN PRESS

growth responses, ranging from parental-like to reduced or, depending on the stressor, improved growth performance. For clarity, the complete growth dataset for all the 30 MSCs is reported in the *Supplementary Materials* (**Table S1**). Based on this preliminary screening, six representative MSCs per stressor were selected for detailed growth characterization, as previously described (Material and Methods, 2.7 paragraph).

3.1.1 Growth response to formic acid (EC_{50} = 3 g L^{-1})

At the formic acid EC_{50} concentration (3 g L^{-1}), growth was uniformly constrained, leading to reduced biomass accumulation across all MSCs at 24 h (**Figure 1B**). Under weak-acid stress, the parental strain consistently displayed the highest growth, whereas all monosporal cultures exhibited comparable or lower growth profiles. Relative growth data (Supplementary Materials, **Table S1**), identified MSC14 and MSC48 as the closest to the parental phenotype, reaching 80% and 77% relative growth, respectively. In contrast, MSC3 (42%) and MSC44 (50%) were the most severely affected by formic acid, whereas MSC33 (67%) and MSC70 (64%) displayed intermediate phenotypes. Overall, formic acid elicited graded growth reductions across MSCs, with no isolates outperforming the parental strain. This pattern is aligned with the mechanism of action of weak organic acids, which primarily challenge intracellular pH homeostasis and increase the energetic cost of proton extrusion [35], thereby making growth largely dependent on the ability to maintain cellular homeostasis rather than on gains in metabolic efficiency. Accordingly, although sporulation revealed quantitative differences in growth impairment among MSCs, formic acid imposed a strong growth-limiting constraint that restricted phenotypic diversification compared with the more heterogeneous responses observed under the other stress conditions tested.

ARTICLE IN PRESS

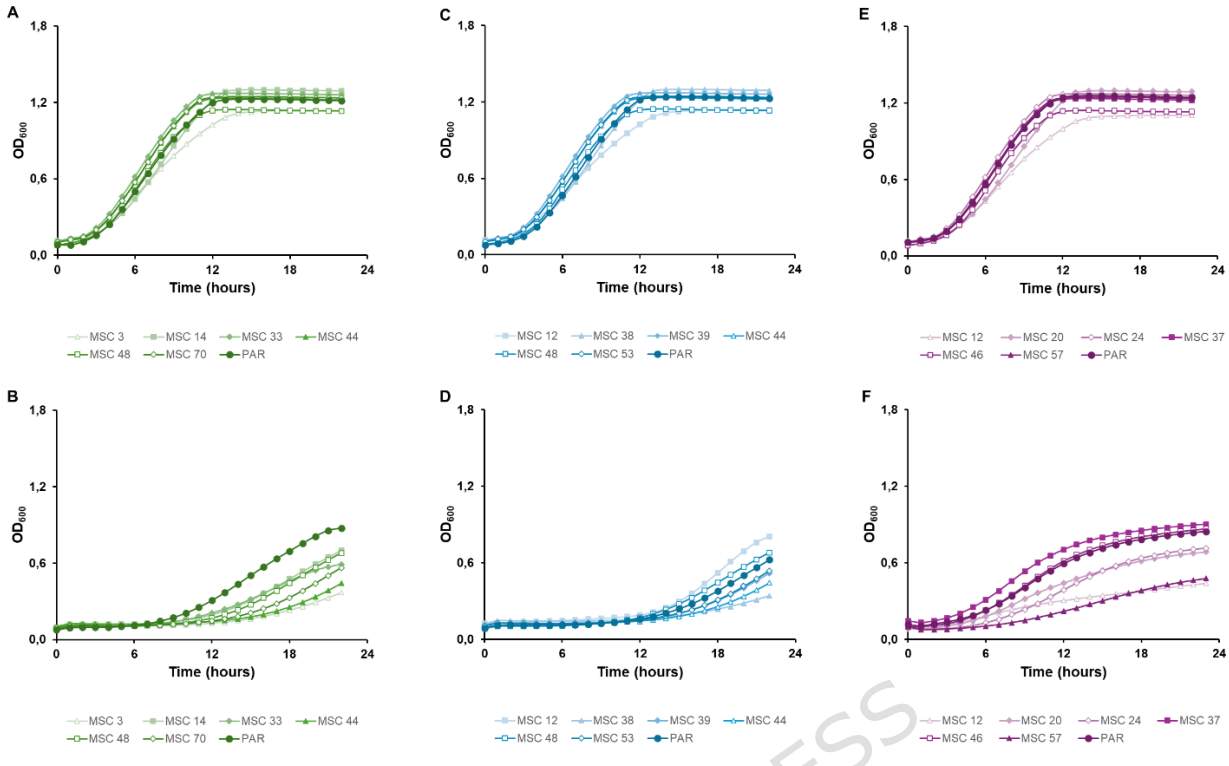

Figure 1. Growth curves of selected MSCs under different stress conditions.

Mean growth curves are shown for monosporal colonies cultivated in the presence of formic acid (panels A-B), furfural (panels C-D), and sodium chloride (panels E-F). Panels A, C, and E represent control conditions in glucose-containing synthetic defined medium, while panels B, D, and F correspond to cultures exposed to the respective stressors. Growth was monitored by optical density (OD_{600}) measurements over time, and curves represent mean values obtained from biological triplicates.

3.1.2 Growth response to furfural (EC_{50} = 3 g L^{-1})

Growth at the furfural EC_{50} concentration (3 g L^{-1}) revealed a culture-dependent growth response among the selected monosporal colonies (**Figure 1D**). The initial lag phase was comparable across MSCs, whereas clear differences were observed during the exponential growth and in the final cellular densities detected (OD_{600} values). Relative growth at 24 h, expressed as percentage of that of the parental strain (**Table S1**), showed that MSC12 (129%) and MSC48 (109%) outperformed the parental strain in both growth rate and final biomass.

ARTICLE IN PRESS

MSC53 (86%) and MSC39 (83%) displayed growth profiles comparable to the parental, whereas MSC44 (71%) and MSC38 (55%) exhibited reduced growth, with slower kinetics and lower final OD_{600}. Furfural is widely reported to impair growth primarily by disrupting cellular redox balance and inhibiting metabolic activity, leading mainly to delayed growth kinetics rather than a marked reduction in final biomass accumulation [36]. Consistent with this mode of action, growth differences among monosporal colonies reflected variable efficiency in coping with furfural stress. The superior performance of MSC39 and MSC12 suggests enhanced stress response capacity, whereas MSC38 and MSC53 appear more sensitive. MSC44 and MSC48 displayed an intermediate phenotype comparable to the parental strain. Overall, furfural stress revealed intrinsic phenotypic variability, allowing the identification of isolates with higher or lower tolerance than the parental strain.

3.1.3 Growth response to sodium chloride (EC_{50} = 50 g L^{-1})

Growth at the NaCl EC_{50} concentration (50 g L^{-1}), remained largely sustained across cultures, with well-defined exponential phases and substantial biomass accumulation (**Figure 1F**). Under salt stress, MSC37 and MSC46 grew slightly over the parental (107%, 103%), whereas MSC24 and MSC20 showed moderate reductions (84%, 81%). By contrast, MSC57 (57%) and MSC12 (52%) exhibited delayed kinetics and reduced final cell density. Sodium chloride primarily imposes stress by inducing osmotic and ionic imbalance. As a result, survival and growth depend mainly on restoring osmotic balance and maintaining ion homeostasis, rather than on systems for enzymatic detoxification of a reactive toxic molecule as required for inhibitors such as furfural [37]. The observed growth differences among monosporal cultures therefore likely reflect variation in the efficiency of osmotic adaptation rather than intrinsic limitations in metabolic capacity. Accordingly, NaCl stress revealed quantitative differences in adaptive efficiency within the population, contrasting with the growth-limiting constraint

ARTICLE IN PRESS

imposed by formic acid and the heterogeneous, detoxification-driven responses observed under furfural stress.

Overall, the three stressors elicited distinct OD_{600} profiling, in line with their specific mechanisms of action. Formic acid seemed to impose a stringent energetic burden that may have limited growth improvements beyond the parental phenotype. Furfural primarily affected growth kinetics, revealing pronounced phenotypic heterogeneity and the emergence of high-performing isolates. By contrast, sodium chloride mainly shifted growth performance across isolates, potentially reflecting differences in osmotic adaptation efficiency, without generating extreme phenotypes.

3.2 Stress tolerance in Ethanol Red and derived monosporal cultures

The six MSCs, selected according to phenotypes similar to, higher than or lower than that of the parental *S. cerevisiae* ER strain, were further investigated by FTIR bioassay and viability assessment following exposure at high cell density to the EC_{50} of each individual inhibitor. CFU-based plate counts revealed a clear stressor-dependent effect on cultivability and survival of both parental and derived MSCs (**Table 1**).

ARTICLE IN PRESS

In the parental strain, a moderate effect was observed upon exposure to formic acid (FC = 0.47; 53% mortality), whereas furfural caused the strongest reduction in cultivability (FC = 0.28), corresponding to a mortality of 72%. By contrast, sodium chloride had a limited impact, with high residual cultivability (FC = 0.88; 12% mortality).

Table 1. CFU-based cultivability and mortality of the parental *S. cerevisiae* strain Ethanol Red and the selected monosporal cultures (MSCs) under stress**.**

Stressor	Culture	Control CFU (mL^{-1}) mean ± SD	Test CFU (mL^{-1}) mean ± SD	Mortality (%)	FC
Formic Acid	**Par**	4.33E+08 ± 2.52E+07	2.05E+08 ± 5.51E+06	**53**	0.47
	14	1.80E+10 ± 1.80E+10	5.30E+09 ± 1.80E+10	**71**	0.29

ARTICLE IN PRESS

	03	8.97E+08	±	8.74E+07	7.60E+08	±	2.00E+07	**15**	0.85
	33	2.00E+09	±	1.53E+07	2.33E+08	±	1.10E+07	**88**	0.12
	44	2.35E+09	±	4.04E+07	3.50E+08	±	1.00E+07	**85**	0.15
	48	1.66E+09	±	2.00E+07	1.23E+08	±	5.51E+06	**93**	0.07
	70	1.77E+09	±	4.04E+07	4.53E+08	±	2.08E+07	**74**	0.26
Furfural	**Par**	7.83E+08	±	1.00E+08	2.20E+08	±	1.53E+06	**72**	0.28
	12	1.24E+09	±	2.00E+07	2.44E+08	±	2.12E+07	**80**	0.20
	38	6.87E+08	±	1.53E+07	1.31E+08	±	1.00E+07	**81**	0.19
	39	3.26E+09	±	2.85E+08	9.60E+08	±	5.57E+07	**71**	0.29
	44	4.50E+08	±	2.00E+07	1.75E+08	±	8.00E+06	**61**	0.39
	48	3.50E+08	±	2.00E+07	1.59E+08	±	2.00E+07	**55**	0.45
	53	4.50E+08	±	1.00E+07	3.50E+08	±	1.00E+07	**22**	0.78
Sodium	**Par**	2.52E+08	±	4.00E+07	2.21E+08	±	5.00E+07	**12**	0.88
chloride	12	2.28E+08	±	3.79E+07	1.40E+08	±	1.37E+07	**39**	0.61
	24	2.54E+08	±	3.61E+07	1.03E+08	±	2.31E+07	**59**	0.41
	35	3.00E+08	±	8.50E+06	2.26E+08	±	1.72E+07	**25**	0.75
	37	2.04E+08	±	1.40E+07	1.44E+08	±	1.25E+07	**30**	0.70
	43	2.71E+08	±	4.51E+07	2.16E+08	±	1.55E+08	**20**	0.80
	57	2.09E+08	±	2.52E+07	2.04E+08	±	3.06E+07	**2**	0.98

Legend. Cells were cultivated for 4 h in YNB + 2% (w/v) glucose and then exposed for 4 h to formic acid (3 g L^{-1}), furfural (3 g L^{-1}) or sodium chloride (50 g L^{-1}). Cultivability was assessed by plate counting and expressed as CFU m L^{-1} (mean ± SD). Control CFU and Test CFU refer to unstressed and stressed conditions, respectively. **Mortality (%)** was calculated as [1 – (CFU_{test} / $CFU_{control}$)] x 100. The fold change column (FC) reports the relative cultivability of

ARTICLE IN PRESS

each culture under stress, calculated from plate counts as CFU_{test} / $CFU_{control}$): **FC = 1** indicates no change; **FC > 1** increased cultivability; **FC < 1** decreased cultivability.

After 4 h exposure to formic acid (3 g L^{-1}), most MSCs displayed a pronounced loss of cultivability, with mortality values exceeding 70% and fold changes (FC) ≤ 0.29 in five out of the six MSCs tested. MSC 48 was the most sensitive culture (93% mortality), followed by MSC33 (88%), MSC44 (85%), MSC70 (74%) and MSC14 (71%), whereas MSC3 retained substantially higher tolerance (FC = 0.85; 15% mortality). This pattern is in line with the known inhibitory effects of weak acids in yeast, which have been associated with intracellular acidification and increased ATP demand to restore pH homeostasis, thereby rapidly reducing cultivability when compensatory responses are not sufficient [38]. However, in the present study, CFU-based measurements directly demonstrate differences in cultivability and mortality, while the intracellular mechanisms underlying these differences remain to be specifically investigated. Accordingly, the markedly improved survival of MSC3 indicates a higher tolerance to formic acid under the tested conditions. This phenotype may be compatible with more efficient homeostatic responses to weak-acid stress, but targeted analyses would be required to identify the underlying cellular processes. Exposure to furfural (3 g L^{-1}) resulted in pronounced heterogeneity in the response of the selected MSCs. MSC12 and MSC38 were the most affected (FC = 0.20 and 0.19; 80% and 81% mortality), whereas MSC53 retained the highest tolerance (FC = 0.78; 22% mortality). MSC48 and MSC44 exhibited intermediate sensitivity (FC = 0.45 and 0.39; 55% and 61% mortality) whereas MSC39 displayed a response comparable to that of the parental strain (FC = 0.29; 71% mortality). The broader heterogeneity detected in the MSCs response to furfural stress is in line with furfural activity, playing primarily as a redox stressor. Detoxification relies on NAD(P)H-dependent reduction, so tolerance is expected to scale with a strain's ability to preserve reducing equivalents and manage downstream stress propagation [15,21,38]. Moreover, furfural has been shown to

ARTICLE IN PRESS

promote genome instability (e.g., chromosomal alterations and loss of heterozygosity), which could further amplify phenotypic diversification among derived MSCs [28].

Under osmotic stress induced by NaCl (50 g L^{-1}), the parental strain maintained high cultivability (FC = 0.88; 12% mortality), consistent with robust osmoadaptation programs centered on the high osmolarity glycerol (HOG) pathway and glycerol-based osmoregulation. The divergent MSCs profiles likely reflect differences in the efficiency of these osmo-protective responses [39,40]. MSC57 was the most tolerant (FC = 0.98; 2% mortality), followed by MSC43 (FC = 0.80; 20% mortality) and MSC35 (FC = 0.75; 25% mortality). The strongest reduction in tolerance was detected in MSC12 (FC = 0.61; 39% mortality) and MSC24 (FC = 0.41; 59% mortality).

3.3 FTIR signatures reveal stressor-specific biochemical remodeling in MSC cultures

To quantify stress-associated spectral divergence, an unsupervised multivariate overview by PCA on normalized FTIR spectra was first performed and then assessed parental vs. MSC differences by wavelength-wise comparisons under each condition (**Figure 2**). PCA explained a substantial fraction of the spectral variance (66.1%), with PC1 and PC2 accounting for 43.0% and 23.1%, respectively (**Figure 2A**). The widest dispersion was observed under furfural exposure, whereas NaCl-treated profiles showed extensive overlap with controls. Along PC1, furfural (Fu) and, to a lesser extent, formic acid (Fa) samples tended to score at positive PC1 values, whereas controls (C) and NaCl (N) samples clustered predominantly at negative to near-zero PC1 values. PC2 further captured within-stressor heterogeneity, which was most pronounced under furfural, as reflected by the broad spread of Fu scores and the largest 95% confidence ellipse, consistent with marked strain-to-strain variability in this condition.

ARTICLE IN PRESS

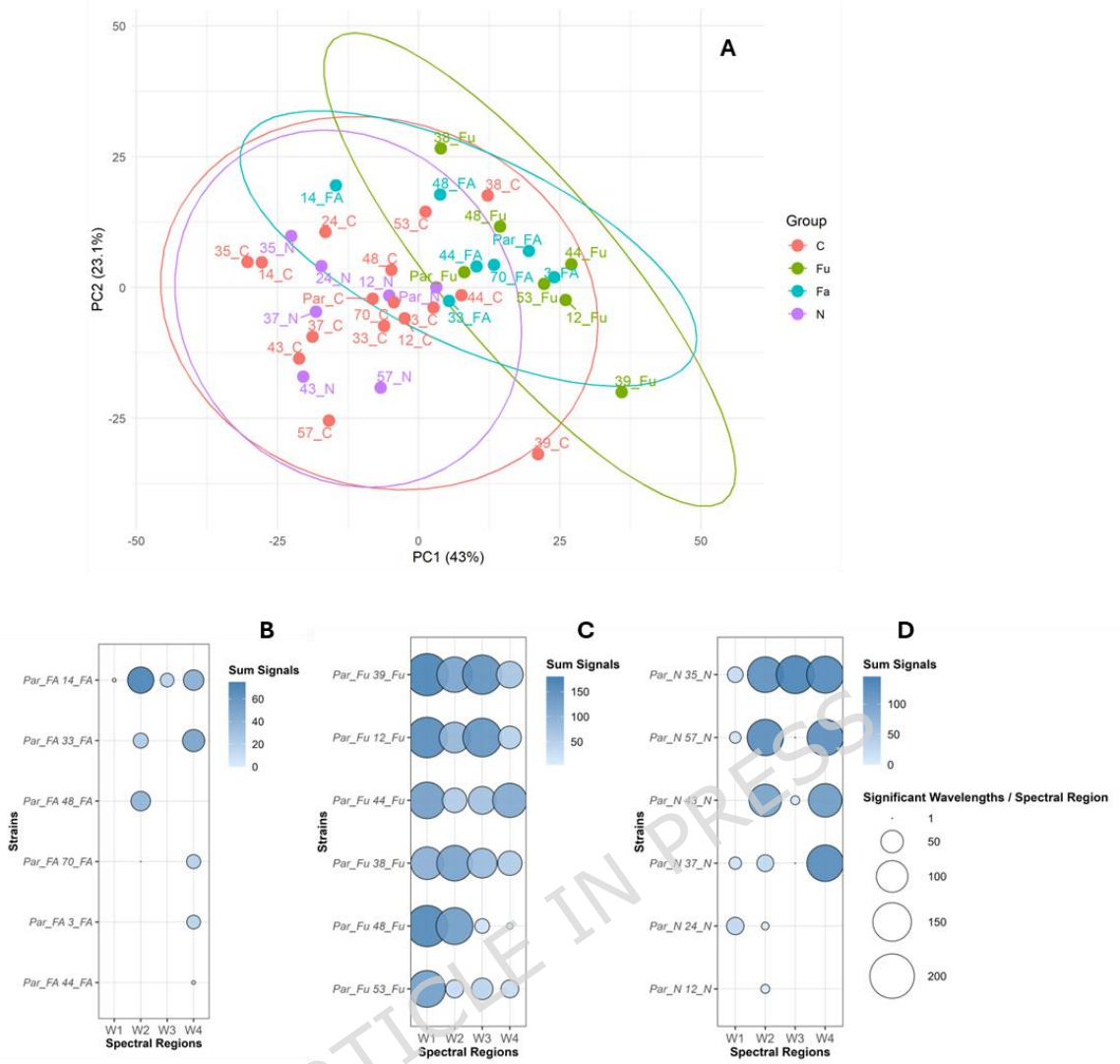

ARTICLE IN PRESS

Figure 2. PCA and region-resolved FTIR spectral divergence between parental and MSCs cultures under stress. (**A**) PCA score plot of normalized FTIR spectra from cultures under control conditions (C) and after 4 h exposure to formic acid (Fa, 3 g L^{-1}), furfural (Fu, 3 g L^{-1}) or sodium chloride (N, 50 g L^{-1}). PC1 (43.0%) vs PC2 (23.1%) explains 66.1% of total variance. Points represent mean spectra (3 biological replicates x 3 technical replicates); ellipses denote 95% confidence regions. (**B**–**D**) Bubble plots summarizing parental *vs*. MSCs spectral divergence under (**B**) formic acid, (**C**) furfural and (**D**) sodium chloride. For each parental–MSC pair, spectra were compared at each wavenumber using a two-tailed Student's t-test. *p*-values were adjusted for multiple testing using FDR and significant wavenumbers (FDR-

ARTICLE IN PRESS

adjusted $p < 0.01$) were counted within four spectral windows, namely fatty acids (W1), amides (W2), mixed (W3) and carbohydrates (W4).

Guided by the clustering provided by PCA, the spectral divergences between parental and MSCs under each stressing condition were then mapped at higher resolution. More in detail, parental and MSCs spectra were compared in pairs at each wavenumber using independent two-tailed Student's t-tests and the number of significantly different wavelengths ($p < 0.01$) was subsequently summarized within spectral windows from W1 to W4 (**Figure 2B**, **2C**, **2D**). Overall, the extent and the distribution of significant differences were stressor-specific. Under formic acid (**Fig. 2B**), spectral divergence from the parental strain was limited and primarily confined in W2, with a secondary contribution from W4. MSC14 showed the strongest overall deviation, with significant differences distributed across the spectrum but dominated by W2. Differences in W2 were also evident for MSC48 and MSC33. In contrast, W4 changes were most pronounced in MSC 33 and MSC14, with weaker effects observed for MSC70 and MSC3. Except for a few wavelengths in W4, no significant differences were detected for MSC44 relative to the parental strain.

Under furfural stress (**Fig. 2C**), all MSCs displayed FTIR profiles that differed significantly from the parental strain, indicating a marked divergence in response to this stressor. A high density of significant different wavenumbers was detected across all spectral windows, with the response consistently dominated by lipid, protein/amides and mixed-region bands (W1-W3), whereas carbohydrate-associated bands contributed to a lesser extent in most comparisons. The largest divergences were observed for MSC39 and MSC12, which displayed extensive differences spanning the full spectrum, with particularly strong contributions in W1 and W3. MSC44 and MSC38 also exhibited broad, region-wide changes, with MSC44 characterized by a comparatively higher contribution from W4. In contrast, MSC48 exhibited a more region-restricted pattern, with differences largely confined to W1-W2 and markedly

ARTICLE IN PRESS

reduced contributions in W3-W4. MSC53 showed an intermediate profile dominated by W1 and with fewer significant features in the remaining regions.

Compared with the differences detected under formic acid and furfural exposure, sodium chloride elicited a moderate, region-dependent remodeling of the FTIR fingerprints, mainly involving W2 and W4 (**Fig. 2D**). MSC35 exhibited the most extensive response, with numerous significant differences spanning W2-W4 and only a minor contribution from W1. A similar but less pronounced profile was detected for MSC57 and MSC43, where changes were concentrated mainly in W2 and W4 with a limited involvement of W3. Conversely, MSC37 displayed a region-specific pattern dominated by W4, consistent with NaCl-associated alterations primarily affecting carbohydrate-related spectral features. MSC24 showed only modest divergence, with few significant differences largely restricted to earlier spectral windows, whereas MSC12 exhibited minimal changes, confined to a narrow signal in W2.

MSCs evaluated under different stressors, namely MSC 44 and MSC 48 under formic acid and furfural and MSC 12 under furfural and sodium chloride, exhibited stressor-specific FTIR signatures, with consistent shifts in both the magnitude and regional distribution of the significant detected differences.

ARTICLE IN PRESS

3.4 FTIR spectral remodeling under stress

To further investigate the spectral differences between the parental strain and the selected MSCs under each stress condition, we focused on the subset of FTIR wavenumbers showing significant changes (FDR-adjusted $p < 0.05$). These features were used to identify discriminant peaks describing MSC-specific fingerprint shifts relative to the parental strain [34,41]. Peaks are reported together with the relative cultivability of each MSC, calculated from plate counts under the same stress condition as the ratio CFU_{MSC} / CFU_{par}. Overall, divergences from the parental strain under stress were captured by recurrent peaks associated with lipids (3020-2800

ARTICLE IN PRESS

cm^{-1} and 1500-1300 cm^{-1}), proteins (1700-1500; 1300 cm^{-1}), polyphosphates, phospholipids and nucleic acids (1300-1200 cm^{-1}) and carbohydrates (1200-800 cm^{-1}) (**Table 2**, **Table 3**).

It should be emphasized, however, that FTIR fingerprinting provides a whole-cell biochemical profile of stress-associated remodeling rather than direct causal identification of the molecular mechanisms underlying the observed phenotypes. Accordingly, the spectral differences reported here should be interpreted as descriptive biochemical signatures associated with stress response, with band assignments providing functional indications rather than mechanistic evidence.

3.4.1 Formic acid exposure

After 4 h exposure to formic acid (3 g L^{-1}), mortality exceeded 70% in all MSCs, except for MSC3 (15%) (**Table 1**). When benchmarked against the parental strain, most MSCs showed a relative advantage, with FC values above 1, while MSC48 performed worse (FC = 0.60) (**Table 2**).

Table 2. Stress-specific FTIR band shifts and relative cultivability in paired parental - MSC comparisons.

Stressor	MSCs	Lipids		Proteins					Polyphosph Phospholip Nucleic ac
		3020-2800	1500-1300	1700-1500; 1300					1300-120
Formic acid	MSC 33	ns	↑1456	↓1654	↓1544	↑1400	↑1307	↑1296	↑1247
	MSC 14	↓2928	↑1456	↑1654	↑1546	↑1400	ns	↑1296	↑1247
	MSC 48	ns	ns	↑1654	ns	ns	ns	ns	ns
	MSC 3	ns	ns	ns	ns	ns	ns	ns	ns
	MSC 44	ns	ns	ns	ns	ns	ns	ns	ns
	MSC 70	ns	ns	ns	ns	ns	ns	ns	ns
Furfural	MSC 53	ns	↓1451	↓1654	↓1544	↓1399	↓1305	ns	↓1247
	MSC 12	↑2926	↓1451	↓1654	↓1544	ns	↓1305	ns	↓1247
	MSC 48	↑2926	↑1451	↑1652	↑1544	ns	ns	ns	↑1247
	MSC 38	↑2926	↑1451	ns	ns	ns	ns	↑1295	↑1245
	MSC 39	↑2926	↓1451	↓1654	↓1544	↓1399	↓1305	ns	↓1247
	MSC 44	↑2926	↓1451	ns	ns	↓1399	↓1305	ns	↓1247
	MSC 12	ns	ns	ns	ns	ns	ns	ns	ns

ARTICLE IN PRESS

Sodium chloride	**MSC 24**	↓2926	ns	↑1654	ns	ns	ns	ns	ns
	MSC 35	ns	↑1453	↑1650	↑1542	↑1399	↑1307	ns	↑1243
	MSC 37	↓2926	↑1451	↓1654	ns	↑1399	↑1309	ns	↑1245
	MSC 43	ns	ns	↓1654	↓1544	ns	↑1310	ns	ns
	MSC 57	ns	ns	↓1654	↓1544	ns	ns	ns	ns

Legend. Significant wavenumbers are reported within spectral windows as band positions (cm^{-1}). For each paired comparison (**MSC vs parental**), arrows indicate the direction of the change in band intensity (two-tailed Student's t-test with FDR correction; FDR-adjusted $p < 0.05$): ↑ higher intensity in MSC than in parental; ↓ lower intensity in MSC; ns, no significant differences. The fold change column (**FC**) reports the relative cultivability of each MSC compared with the parental strain under the same stress condition, calculated from plate counts as CFU_{MSC}/ CFU_{par}. FC = 1 indicates no change; FC > 1 increased cultivability; FC < 1 decreased cultivability.

Table 3. Peak assignment of bands in FTIR spectra.

Absorption band (cm^{-1})	**Peak assignment**	**Main biomolecules**	**Assigned effect**
~2925	ν_{asym} CH_2 of acyl chains	Lipids and Proteins	Remodeling and/or da the yeast cell membra parental strain
1680-1640	Amide I band (C=O stretching)	Proteins	Protein structural rear bond in different prote
1580–1520	Amide II (bending vibration of N–H and the stretching vibration of C–N)		
~1455	Various CH_2/CH_3 bending vibrations	Lipids and Proteins	Protein and lipid rearr
~1390	C═O of COO− symmetric stretching	Proteins	Protein structural rear
~1300	Amide III: C−N and C−O stretching, N−H and O═C−N bending		
~1240	ν_{asym} PO^{2-}	DNA, RNA and membrane phospholipids	Degradation of nucleic consequent increase o
~1080	ν_{sym} PO^{2-}	RNA and membrane phospholipids	
~1060	C–O and C–C stretching, C–O–H and C–O–C deformation	Carbohydrate and polysaccharide components: chitin	Degradation of nucleic consequent increase o
~1050	Mannans	Major parietal polysaccharides: mannans	

ARTICLE IN PRESS

FTIR changes were largely limited to MSC14 and MSC33, whereas the other MSCs showed either minimal change, MSC48 showed a single discriminant peak at 1654 cm^{-1} (Amide I), or no discriminant bands (MSC3, MSC44 or MSC70). MSC14 and MSC33 shared almost the same set of discriminant peaks with several bands showing an opposite trend between the two cultures. Amide I and Amide II bands (1654 cm^{-1} and ~1555 cm^{-1}) increased in MSC14 and decreased in MSC33 while cell-wall chitin band at 1060 cm^{-1} decreased in MSC14 and increased in MSC33. In contrast, both cultures displayed enhanced signals around 1300 cm^{-1} (Amide III), 1456 cm^{-1} (CH_2-CH_3 bending vibrations from lipids and proteins), 1400 cm^{-1} (COO^- vibrations in protein) and 1247 cm^{-1} (ν_{sym} PO_2^- in membrane phospholipids), indicating a shared response compatible with phospholipid modulation coupled to protein conformational rearrangements under formic acid stress. In addition, MSC33 showed an increase at 1078 cm^{-1}, consistent with changes interesting intracellular nucleic acids and/or phospholipid-associated contributions whereas MSC14 was the only culture showing a distinct modulation of membrane lipid features relative to the parental strain (2928 cm^{-1}) (**Table 3)**.

Overall, these data indicate a culture-specific response to formic acid. MSC14 combined a significant increase in cultivability (FC = 25.85) with a distinctive FTIR profile showing changes in spectral regions commonly assigned to cell-envelope components and protein conformational rearrangements, whereas MSC33 showed extensive remodeling across amide, phosphate and carbohydrate regions but only a modest gain in cultivability (FC = 1.14) compared with the parental strain. These signatures are consistent with the known effects of weak-acid stress, which have been associated with intracellular acidification, increased ATP demand for pH homeostasis and downstream effects on envelope integrity and protein homeostasis [26,38,42].

3.4.2 Furfural exposure

ARTICLE IN PRESS

After 4 h exposure to furfural (3 g L^{-1}), MSCs displayed marked heterogeneity in viability, relative cultivability and FTIR biochemical profiles (**Tables 1, Table 2**). Mortality ranged from 22% in MSC53 to 80-81% in MSC12 and MSC38, with intermediate values for MSC48 (55%), MSC44 (61%) and MSC39 (71%). Relative cultivability also varied across MSCs: three outperformed the parental strain, whereas three showed reduced cultivability under furfural stress.

The spectral divergences in response to furfural stress are dominated by lipid-associated changes. The band assigned to the asymmetric stretching of CH_2 of acyl chains (2926 cm^{-1}) increased in all MSCs except MSC53. The second lipid-associated marker at 1451 cm^{-1} (CH_2-CH_3 bending) showed two opposite trends, with increased intensity only in MSC48 and MSC38, possibly reflecting differences in lipid-associated spectral features that may be linked to membrane lipid packing or composition in MSC cultures. Amides and protein associated changes were heterogeneous and did not mirror the uniform lipid signal (1654 cm^{-1}, 1544 cm^{-1}, 1399 cm^{-1}, ~1300 cm^{-1}) (**Table 3**). The modulation of the phosphate-related band at 1247 cm^{-1}, commonly assigned to phosphate-containing cellular components such as phospholipid headgroups and phosphodiester moieties in nucleic acids, varied across MSCs with neither correlation with mortality. This arrangement can reflect differences in membrane headgroup exposure/packing or phosphate-domain remodeling, since PO_2^- vibrations are very sensitive to the local chemical environment (e.g., hydrogen bonding and hydration) [43]. Finally, furfural induced a significant shift in the cell-wall carbohydrate band (1077 cm^{-1}), consistently accompanied by a shift in the 1050 cm^{-1} band assigned to cell-wall mannans, with MSC53 as the sole exception. Taken together, these patterns identify a conserved envelope-remodeling signature across MSCs in response to furfural, best interpreted as a robust marker of exposure rather than a primary determinant of tolerance. Accordingly, the prominent lipid-associated signal may be linked to membrane-level responses occurring during furfural exposure. Based

ARTICLE IN PRESS

on previous evidence, membrane integrity, together with the ability to maintain redox balance and activate stress defense systems, may contribute to survival and cultivability in yeast exposed to furfural [44-46].

3.4.3 Sodium chloride exposure

Out of the three tested stressing agents, sodium chloride imparted the lowest mortality, ranging from 2% in MSC57 to 59% in MSC24, with all other cultures remaining below 40%. Nevertheless, cultivability generally reduced (FC = 0.47 - 0.97), indicating that most MSCs were more sensitive than the parental background, with MSC35 as the only isolate maintaining parental-like performance (FC = 1.02). FTIR remodeling was MSC dependent and mainly involved spectral divergences in regions commonly assigned to biochemical features potentially related to cell-envelope remodeling and stress response, including lipid-associated bands (2926 cm^{-1}; ~1450 cm^{-1}), amide and protein bands (~ 1650 cm^{-1}; ~ 1540 cm^{-1}, 1390 cm^{-1}; 1300 cm^{-1}) and phosphate-related features (~ 1240 cm^{-1}; ~ 1080 cm^{-1}) (**Table 3**). MSC35 showed the broadest response, with increased signals at 1453 cm^{-1}, 1650 cm^{-1}, 1542 cm^{-1}, 1399 cm^{-1}, 1307 cm^{-1}, 1243 cm^{-1} and 1073 cm^{-1} whereas MSC12 showed no significant discriminant peaks under NaCl despite reduced cultivability (FC = 0.63) (**Table 2)**. Such patterns are consistent with canonical yeast osmotic-stress physiology, where osmoadaptation is coordinated by the High Osmolarity Glycerol (HOG) pathway and relies on ion homeostasis and glycerol-centered responses that impose a substantial homeostatic burden and can impact membrane properties and protein stability [34,39]. In line with the central role of membrane organization in salt tolerance, MSCs showing lipid-region modulation (2926 cm^{-1}; ~1450 cm^{-1}) likely reflect changes in acyl-chain packing and/or membrane composition, which are known to shift under salt stress and to influence tolerance [40,41]. Likewise, variability in the phosphate band near 1240-1250 cm^{-1} may be linked to differences in the phospholipid headgroup environment, since phosphate stretching modes are highly sensitive to local

ARTICLE IN PRESS

hydration state and headgroup interactions in model membranes [47]. Overall, the NaCl dataset indicates that most MSCs were more sensitive than the parental strain under the tested osmotic-stress condition. In parallel, FTIR fingerprints revealed MSC-dependent differences in spectral regions commonly associated with lipid- and protein-related features, suggesting a possible link between differential NaCl sensitivity and culture-specific modulation of membrane-associated and protein-associated responses during osmotic stress.

Taken together, these findings indicate that sporulation-based diversification can reveal stress-dependent phenotypic variability even within a highly domesticated industrial yeast background. However, the observed responses also highlight that the effectiveness of this approach strongly depends on the genetic architecture of the parental strain and requires extensive downstream screening to identify industrially relevant derivatives. Therefore, sporulation should be considered a complementary exploratory strategy for strain improvement rather than a replacement for targeted approaches.

4. Conclusions

This study reported for the first time that sporulation of a highly domesticated, heterothallic industrial yeast can give rise to measurable, reproducible, and stress-dependent phenotypic variability. Despite the heterothallic nature and presumed genomic stability of the parental strain, the analyzed subset of mono-spore derivatives displayed measurable displayed measurable variability not only under industrially relevant stressors (formic acid, furfural, NaCl) but also under standard glucose conditions, indicating that sporulation can unlock latent functional heterogeneity. FTIR fingerprinting demonstrated that sporulation-derived diversity is mirrored at the biochemical level, with patterns that were both stressor-specific and strain-specific. Formic acid responses involved coordinated modulation of protein and membrane features, furfural responses were dominated by lipid-associated signatures and NaCl responses

ARTICLE IN PRESS

reflected membrane and osmotic homeostasis adjustments. These data indicate that MSCs diversification is not merely quantitative but reflects distinct cellular reprogramming strategies. Although the reproducibility of the growth, cultivability and FTIR profiles supports the occurrence of stable phenotypic diversification among monosporal cultures, the present study does not directly establish the genetic basis of this variability. Epigenetic or physiological contributions cannot be excluded. To address this limitation, whole-genome sequencing and comparative genomic analyses of selected high- and low-performing MSCs are currently ongoing in our laboratories. These analyses will be essential to determine whether the observed phenotypes are associated with meiotic segregation of hidden heterozygosity, loss of heterozygosity, copy-number variation, structural variants or other sporulation-associated genome-level changes.

Collectively, these findings support the concept that sporulation can act as a mechanism of functional reshuffling even in long-domesticated industrial strains. Further integration of genomic data with FTIR profiling and targeted phenotypic validation will help clarify the molecular basis of stress-specific remodeling and support the identification of candidate genetic determinants for the development of yeast strains with improved resistance to industrially relevant stressors.

ARTICLE IN PRESS

Supplementary Information

Table S1.xlsx Mean OD_{600} values of the parental strain and MSCs monitored at 1 h intervals over 24 h under control conditions and in the presence of the indicated stressors.

Table S2, S3, S4.xlsx Normalized FTIR spectra of the parental strain and MSCs under control conditions and after 4 h exposure to each stressor.

Figure S1.ppt FTIR fingerprints under formic acid stress. Normalized mean FTIR spectra of the parental strain and selected MSCs after 4 h exposure to formic acid (3 g L^{-1}).

ARTICLE IN PRESS

Figure S2.ppt FTIR fingerprints under furfural stress. Normalized mean FTIR spectra of the parental strain and selected MSCs after 4 h exposure to furfural (3 g L^{-1}).

Figure S3.ppt FTIR fingerprints under sodium chloride stress. Normalized mean FTIR spectra of the parental strain and selected MSCs after 4 h exposure to NaCl (50 g L^{-1}).

Acknowledgments

Not applicable.

Author contributions

Viviana Paulon Writing: original draft, Visualization, Methodology, Investigation, Formal analysis; **Ameya Pankaj Gupte Investigation**: Formal analysis; **Katarina Stojkov Investigation**: Formal analysis; **Chiara Ruspi**: Investigation: **Debora Casagrande Pierantoni**: Methodology and Formal analysis; **Marina Basaglia**: Writing - review & editing; **Gianluigi Cardinali**: Writing - review & editing, Conceptualization; **Lorenzo Favaro**: Writing - review & editing, Supervision, Funding acquisition, Methodology, Conceptualization; **Laura Corte**: Writing - review & editing, Supervision, Funding acquisition, Methodology, Visualization, Conceptualization.

ARTICLE IN PRESS

Funding

This work was funded by University of Padova [2025DAFNAE1SIDPROGETTI-0001, 2025DAFNAE1DOR-00533].

Data availability

All data generated or analyzed during this study are included in this published article and its supplementary information files.

Declarations

Ethics approval and consent to participate

Not applicable.

Consent for publication

ARTICLE IN PRESS

Not applicable. All the authors agree to the submission and publication of this manuscript.

Competing interests

The authors declare that they have no competing interests.

Bibliography

[1] Attfield PV. Crucial aspects of metabolism and cell biology relating to industrial production and processing of *Saccharomyces* biomass. Crit Rev Biotechnol 2023;43:920–37. https://doi.org/10.1080/07388551.2022.2072268.

[2] Parapouli M, Vasileiadis A, Afendra A-S, Hatziloukas E. *Saccharomyces cerevisiae* and its industrial applications. AIMS Microbiol 2020;6:1–31. https://doi.org/10.3934/microbiol.2020001.

[3] Liu C, Choi B, Efimova E, Nygård Y, Santala S. Enhanced upgrading of lignocellulosic substrates by coculture of *Saccharomyces cerevisiae* and Acinetobacter baylyi ADP1. Biotechnol Biofuels Bioprod 2024;17:61. https://doi.org/10.1186/s13068-024-02510-8.

[4] Steensels J, Gallone B, Voordeckers K, Verstrepen KJ. Domestication of Industrial Microbes. Curr Biol 2019;29:R381–93. https://doi.org/10.1016/j.cub.2019.04.025.

[5] Gallone B, Steensels J, Prahl T, Soriaga L, Saels V, Herrera-Malaver B, et al. Domestication and Divergence of *Saccharomyces cerevisiae* Beer Yeasts. Cell 2016;166:1397-1410.e16. https://doi.org/10.1016/j.cell.2016.08.020.

[6] Favaro L, Jansen T, van Zyl WH. Exploring industrial and natural Saccharomyces cerevisiae strains for the bio-based economy from biomass: the case of bioethanol. Crit Rev Biotechnol 2019;39:800–16. https://doi.org/10.1080/07388551.2019.1619157.

[7] Gupte AP, Pierantoni DC, Conti A, Donati L, Basaglia M, Casella S, et al. Renewing Lost Genetic Variability with a Classical Yeast Genetics Approach. J Fungi 2023;9:264. https://doi.org/10.3390/jof9020264.

ARTICLE IN PRESS

[8] Steensels J, Snoek T, Meersman E, Picca Nicolino M, Voordeckers K, Verstrepen KJ. Improving industrial yeast strains: exploiting natural and artificial diversity. FEMS Microbiol Rev 2014;38:947–95. https://doi.org/10.1111/1574-6976.12073.

[9] Pérez-Través L, Lopes CA, Barrio E, Querol A. Evaluation of different genetic procedures for the generation of artificial hybrids in Saccharomyces genus for winemaking. Int J Food Microbiol 2012;156:102–11. https://doi.org/10.1016/j.ijfoodmicro.2012.03.008.

[10] Sipiczki M. Diversity, variability and fast adaptive evolution of the wine yeast (*Saccharomyces cerevisiae*) genome—a review. Ann Microbiol 2011;61:85–93. https://doi.org/10.1007/s13213-010-0086-4.

[11] Ezov Tk, Chang S-L, Frenkel Z, Segrè Av, Bahalul M, Murray Aw, et al. Heterothallism in *Saccharomyces cerevisiae* isolates from nature: effect of HO locus on the mode of reproduction. Mol Ecol 2010;19:121–31. https://doi.org/10.1111/j.1365-294X.2009.04436.x.

[12] Bai F-Y, Han D-Y, Duan S-F, Wang Q-M. The Ecology and Evolution of the Baker's Yeast *Saccharomyces cerevisiae.* Genes 2022;13:230. https://doi.org/10.3390/genes13020230.

[13] Liti G, Carter DM, Moses AM, Warringer J, Parts L, James SA, et al. Population genomics of domestic and wild yeasts. Nature 2009;458:337–41. https://doi.org/10.1038/nature07743.

[14] Gallone B, Mertens S, Gordon JL, Maere S, Verstrepen KJ, Steensels J. Origins, evolution, domestication and diversity of *Saccharomyces* beer yeasts. Curr Opin Biotechnol 2018;49:148–55. https://doi.org/10.1016/j.copbio.2017.08.005.

[15] Ren J, Zhang M, Guo X, Zhou X, Ding N, Lei C, et al. Furfural tolerance of mutant *Saccharomyces cerevisiae* selected via ionizing radiation combined with adaptive

ARTICLE IN PRESS

laboratory evolution. Biotechnol Biofuels Bioprod 2024;17:117. https://doi.org/10.1186/s13068-024-02562-w.

[16] Zuo F, Wu Y, Sun Y, Xie C, Tang Y. Mechanism of enhanced salt tolerance in Saccharomyces cerevisiae by CRZ1 overexpression. Sci Rep 2024;14:22875. https://doi.org/10.1038/s41598-024-74174-1.

[17] My R, Gupte AP, Bizzotto E, Frizzarin M, Antoniali P, Campanaro S, et al. Unveiling the fitness of *Saccharomyces cerevisiae* strains for lignocellulosic bioethanol: a genomic exploration through fermentation stress tests. New Biotechnol 2025;85:63–74. https://doi.org/10.1016/j.nbt.2024.12.004.

[18] My R, Bizzotto E, Gupte AP, Gallo E, Frizzarin M, Antoniali P, et al. Formic acid resistance in Saccharomyces cerevisiae strains: the role of SAT4 in a proposed molecular model. Bioresour Technol 2026;441:133528. https://doi.org/10.1016/j.biortech.2025.133528.

[19] Palmqvist E, Hahn-Hägerdal B. Fermentation of lignocellulosic hydrolysates. II: inhibitors and mechanisms of inhibition. Bioresour Technol 2000;74:25–33. https://doi.org/10.1016/S0960-8524(99)00161-3.

[20] Greetham D, Zaky AS, Du C. Exploring the tolerance of marine yeast to inhibitory compounds for improving bioethanol production. Sustain Energy Fuels 2019;3:1545–53. https://doi.org/10.1039/C9SE00029A.

[21] Yao L, Jia Y, Zhang Q, Zheng X, Yang H, Dai J, et al. Adaptive laboratory evolution to obtain furfural tolerant *Saccharomyces cerevisiae* for bioethanol production and the underlying mechanism. Front Microbiol 2024;14:1333777. https://doi.org/10.3389/fmicb.2023.1333777.

ARTICLE IN PRESS

ARTICLE IN PRESS

[22] Codón AC, Gasent-Ramírez JM, Benítez T. Factors which affect the frequency of sporulation and tetrad formation in *Saccharomyces cerevisiae* baker's yeasts. Appl Environ Microbiol 1995;61:630–8. https://doi.org/10.1128/aem.61.2.630-638.1995.

[23] Budroni M, Giordano G, Pinna G, Farris GA. A genetic study of natural flor strains of *Saccharomyces cerevisiae* isolated during biological ageing from Sardinian wines. J Appl Microbiol 2000;89:657–62. https://doi.org/10.1046/j.1365-2672.2000.01163.x.

[24] Bahalul M, Kaneti G, Kashi Y. Ether-zymolyase ascospore isolation procedure: an efficient protocol for ascospores isolation in *Saccharomyces cerevisiae* yeast. Yeast 2010;27:999–1003. https://doi.org/10.1002/yea.1808.

[25] Gronchi N, De Bernardini N, Cripwell RA, Treu L, Campanaro S, Basaglia M, et al. Natural Saccharomyces cerevisiae strain reveals peculiar genomic traits for starch-to-bioethanol production: the design of an amylolytic consolidated bioprocessing yeast. Front Microbiol 2021;12:768562. https://doi.org/10.3389/fmicb.2021.768562.

[26] Du C, Li Y, Xiang R, Yuan W. Formate Dehydrogenase Improves the Resistance to Formic Acid and Acetic Acid Simultaneously in *Saccharomyces cerevisiae*. Int J Mol Sci 2022;23:3406. https://doi.org/10.3390/ijms23063406.

[27] Zeng L, Huang J, Feng P, Zhao X, Si Z, Long X, et al. Transcriptomic analysis of formic acid stress response in *Saccharomyces cerevisiae*. World J Microbiol Biotechnol 2022;38:34. https://doi.org/10.1007/s11274-021-03222-z.

[28] Qi L, Zhu Y-X, Wang Y-K, Tang X-X, Li K-J, He M, et al. Nonlethal Furfural Exposure Causes Genomic Alterations and Adaptability Evolution in Saccharomyces cerevisiae. Microbiol Spectr 2023;11:e0121623. https://doi.org/10.1128/spectrum.01216-23.

[29] Favaro L, Cagnin L, Corte L, Roscini L, De Pascale F, Treu L, et al. Metabolomic Alterations Do Not Induce Metabolic Burden in the Industrial Yeast M2n[pBKD2-

ARTICLE IN PRESS

Pccbgl1]-C1 Engineered by Multiple δ-Integration of a Fungal β-Glucosidase Gene. Front Bioeng Biotechnol 2019;7:376. https://doi.org/10.3389/fbioe.2019.00376.

[30] Ruspi C, Casagrande Pierantoni D, Conti A, Scarponi R, Corte L, Cardinali G. Plant Growth-Promoting Yeasts (PGPYs) as a sustainable solution to mitigate salt-induced stress on zucchini plant growth. Biol Fertil Soils 2025;61:293–309. https://doi.org/10.1007/s00374-024-01885-y.

[31] Roscini L, Corte L, Antonielli L, Rellini P, Fatichenti F, Cardinali G. Influence of cell geometry and number of replicas in the reproducibility of whole cell FTIR analysis. Analyst 2010;135:2099–105. https://doi.org/10.1039/C0AN00127A.

[32] Kamrad S, Rodríguez-López M, Cotobal C, Correia-Melo C, Ralser M, Bähler J. Pyphe, a python toolbox for assessing microbial growth and cell viability in high-throughput colony screens. eLife 2020;9:e55160. https://doi.org/10.7554/eLife.55160.

[33] R Core Team. R: A language and environment for statistical computing. Vienna: R Foundation for Statistical Computing; 2024.

[34] Corte L, Roscini L, Pierantoni DC, Pellegrino RM, Emiliani C, Basaglia M, et al. Delta-Integration of Single Gene Shapes the Whole Metabolomic Short-Term Response to Ethanol of Recombinant *Saccharomyces cerevisiae* Strains. Metabolites 2020;10:140. https://doi.org/10.3390/metabo10040140.

[35] Guo Z, Olsson L. Physiological responses to acid stress by *Saccharomyces cerevisiae* when applying high initial cell density. FEMS Yeast Res 2016;16:fow072. https://doi.org/10.1093/femsyr/fow072.

[36] Zhang Z, Xiao D, Wang H, Li Q, Ali S, Chen Y, et al. Enhanced tolerance of *Saccharomyces cerevisiae* to industrial inhibitors through multi-transcription factor engineering for environmental and biotechnological applications. Int Biodeterior Biodegrad 2025;202:106099. https://doi.org/10.1016/j.ibiod.2025.106099.

ARTICLE IN PRESS

ARTICLE IN PRESS

[37] Hohmann S. Osmotic stress signaling and osmoadaptation in yeasts. Microbiol Mol Biol Rev 2002;66:300–72. https://doi.org/10.1128/MMBR.66.2.300-372.2002.

[38] Li B, Liu N, Zhao X. Response mechanisms of *Saccharomyces cerevisiae* to the stress factors present in lignocellulose hydrolysate and strategies for constructing robust strains. Biotechnol Biofuels 2022;15:28. https://doi.org/10.1186/s13068-022-02127-9.

[39] Blomberg A. Yeast osmoregulation – glycerol still in pole position. FEMS Yeast Res 2022;22:foac035. https://doi.org/10.1093/femsyr/foac035.

[40] Chen A, Qu T, Smith JR, Li J, Du G, Chen J. Osmotic tolerance in *Saccharomyces cerevisiae*: Implications for food and bioethanol industries. Food Biosci 2024;60:104451. https://doi.org/10.1016/j.fbio.2024.104451.

[41] Stojkov K, Conti A, Pierantoni DC, Scarponi R, Corte L, Cardinali G. Decoupling Microbial Activity from Metabolite Action: A Comparative Assessment of EM Technology and Its Cell-Free Extract as Nature-Based Solutions for Plant Biostimulation. Horticulturae 2025;11:1528. https://doi.org/10.3390/horticulturae11121528.

[42] Ribeiro RA, Bourbon-Melo N, Sá-Correia I. The cell wall and the response and tolerance to stresses of biotechnological relevance in yeasts. Front Microbiol 2022;13:953479. https://doi.org/10.3389/fmicb.2022.953479.

[43] Arrondo JL, Goñi FM. Infrared studies of protein-induced perturbation of lipids in lipoproteins and membranes. Chem Phys Lipids 1998;96:53–68. https://doi.org/10.1016/s0009-3084(98)00080-2.

[44] Shirvanyan A, Trchounian K. Sodium transport and redox regulation in *Saccharomyces cerevisiae* under osmotic stress depending on oxygen availability. Sci Rep 2024;14:23982. https://doi.org/10.1038/s41598-024-75108-7.

ARTICLE IN PRESS

[45] Sharma SC, Raj D, Forouzandeh M, Bansal MP. Salt-induced changes in lipid composition and ethanol tolerance in *Saccharomyces cerevisiae*. Appl Biochem Biotechnol 1996;56:189–95. https://doi.org/10.1007/BF02786949.

[46] Rodríguez-Vargas S, Sánchez-García A, Martínez-Rivas JM, Prieto JA, Randez-Gil F. Fluidization of membrane lipids enhances the tolerance of *Saccharomyces cerevisiae* to freezing and salt stress. Appl Environ Microbiol 2007;73:110–6. https://doi.org/10.1128/AEM.01360-06.

[47] Binder H, Zschörnig O. The effect of metal cations on the phase behavior and hydration characteristics of phospholipid membranes. Chem Phys Lipids 2002;115:39–61. https://doi.org/10.1016/S0009-3084(02)00005-1.

ARTICLE IN PRESS